ELSEVIER

Journal of Nuclear Materials 296 (2001) 83–89

journal of nuclear materials

www.elsevier.com/locate/jnucmat

Helium production for 0.8–2.5 GeV proton induced spallation reactions, damage induced in metallic window materials

D. Hilscher [a,*], C.-M. Herbach [a], U. Jahnke [a], V. Tishchenko [a], M. Enke [a], D. Filges [b], F. Goldenbaum [b], R.-D. Neef [b], K. Nünighoff [b], N. Paul [b], H. Schaal [b], G. Sterzenbach [b], A. Letourneau [c], A. Böhm [c], J. Galin [c], B. Lott [c], A. Péghaire [c], L. Pienkowski [d]

[a] *Hahn-Meitner-Institut Berlin, Glienickerstr. 100, D-14109 Berlin, Germany*
[b] *Forschungszentrum Jülich, Institut für Kernphysik, D-52428 Jülich, Germany*
[c] *GANIL, IN2P3/CNRS-DSM/CEA, BP 5027, F-14076 Caen, France*
[d] *Heavy Ion Laboratory, Warsaw University, Pl-02-093 Warsaw, Poland*

Abstract

Production cross-sections for neutrons and charged particles as well as excitation energy distributions in spallation reactions were measured recently by the NESSI-collaboration and have been employed to test different intra nuclear cascade models and the subsequent evaporation. The INCL/GEMINI code, which describes best the experimental data has been employed to calculate the damage cross-sections in Fe and Ta as well as the He/dpa ratio as a function of proton energy. For the same amount of neutron production in a typical target of a spallation neutron source the proton beam induced radiation damage in an Fe window is shown to decrease almost linearly with proton energy. For heavier materials such as Ta a similar decrease of the radiation damage is found only for energies above about 3 GeV.

1. Introduction

For future high power spallation neutron sources such as ESS [1] and SNS [2], detailed knowledge of beam induced radiation damage is mandatory in order to estimate lifetimes of materials employed in the target station. This is in particular true for the entrance window of the proton beam separating the radioactive target medium from the accelerator vacuum. The expected radiation-induced damage of materials employed in spallation neutron sources is mainly due to (i) helium gas production and (ii) elastic scattering of neutrons, charged particles, and in particular energetic heavy residues (HR) produced in the spallation process. Helium gas production can cause embrittlement and blistering of metallic materials while the elastic scattering of particles causes changes in the microstructure of materials due to atom displacements/vacancies. The essential contribution to such atom displacements, described by the damage or displacement cross-section σ_d, is due to residual target-like nuclei or HR produced in the spallation reaction. The induced damage is very similar to the one induced by fission fragments.

Compared to the extensively studied radiation damage in fission reactors the damage in spallation neutron sources is characterized by an about 500 times larger ratio of produced helium gas per atom to displacements per atom (He/dpa) [3] in materials which are directly exposed to the incident proton beam. The correlation of both effects – He and dpa – can result in new damage phenomena of mechanical properties. In one year of operation of ESS the produced helium is about 1 or 2.5 at.% for Fe or Ta, respectively, irradiated by 1.3 GeV protons with a uniform beam flux across a diameter of 7 cm at 5 MW, that is an integrated flux of $\phi t = 1.9 \times 10^{22}$ p/cm^2. In order to make simulations for radiation damage of target materials it is important to have a good knowledge of the helium production in spallation

* Corresponding author. Tel.: +49-30 8062 2718; fax: +49-30 8062 2293.
E-mail address: hilscher@hmi.de (D. Hilscher).

0022-3115/01/$ - see front matter
PII: S0022-3115(01)00501-3

reactions. A recent investigation indicated that for helium concentrations below about 0.5–1 at.% no drastic effects on the mechanical properties of steel alloys [4] should occur. On the other hand Maloy et al. [5] reported on changes in the ductility at helium levels far below 0.5 at.%.

Detailed experimental investigations of spallation reactions as a function of proton energies test computer codes, which are needed for the simulation of radiation induced damage of materials employed in the target station. In the following we will discuss particularly the question whether radiation damage can be reduced by changing the incident proton beam energy while keeping the neutron production constant.

2. Comparison of models and data for spallation reactions

Before presenting model calculations describing damage parameters of window materials due to GeV proton induced spallation reactions we confront in the following recently measured thin and thick target data of the NESSI collaboration with predictions obtained with various computer codes.

2.1. Neutron production in thick targets

The essential figure of merit or efficiency of neutron production can be described by the mean number of neutrons (mean neutron multiplicity) produced per incident proton and divided by its energy. This quantity would be constant if the neutron production would increase linearly with incident proton energy. In Fig. 1 this figure of merit is shown as a function of proton energy for lead and tungsten targets for different target geometries. The points display recently measured data [6,7] while the lines are results of calculations with high energy transport codes [8]. We observe an increase of the measured mean neutron number per incident proton and unit energy (expressed in GeV) from 0.1 to about 1 GeV and for higher energies only a slight decrease. The measured data are well described by calculations for a given target geometry and material. By increasing the size of the target to 20 cm diameter and 60 cm length, corresponding to typical target dimensions of a spallation neutron source, the number of neutrons produced increases as well, as indicated in the case of a lead target by the dotted line. We will employ this latter calculation as a reference for the neutron production as a function of incident proton energy between 1 and 4 GeV. The neutron production in a Hg-target of the size proposed for ESS [1] is presumably very similar [6] to this calculated reference from Pb.

While the mean neutron production in thick targets agrees reasonably well with previous data [6] as well as calculations with different transport codes [8] considerable discrepancies are observed for measurements with thin targets, that is for production cross-sections of charged particles.

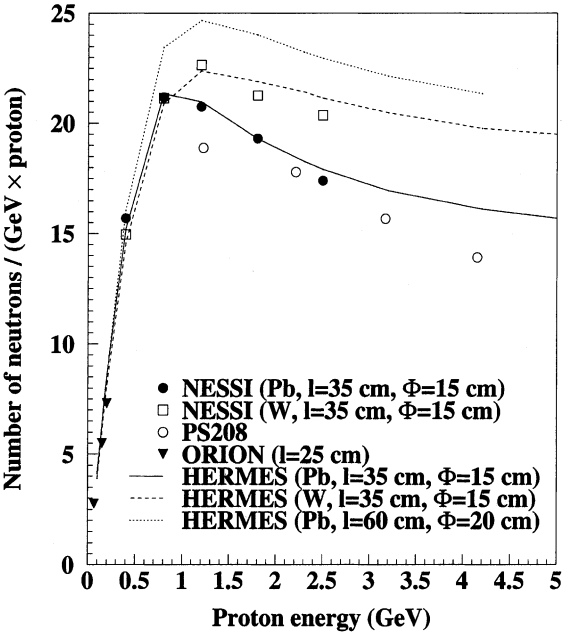

Fig. 1. Average neutron multiplicity per unit beam energy (expressed in GeV) and per incident proton as a function of beam energy for thick Pb and W targets. The targets are cylindrical with a length (l) and diameter (Φ) as indicated. The solid, dotted, and dashed curves are the results of HERMES simulations for Pb: 35 cm × 15 cm ($l \times \Phi$), Pb: 60 cm × 20 cm, and W: 35 cm × 15 cm targets, respectively. The figure has been adapted from [6].

2.2. Charged particle production in thin targets

A compilation of published data [9] for proton induced helium production shows a large dispersion as can be seen in the left panel of Fig. 2 in the case of the spallation reaction p + Fe. That is why the NESSI collaboration had started a campaign to measure the production cross-sections of charged particles for GeV proton induced spallation reactions in thin targets [9,10]. Recent NESSI data are also shown in Fig. 2 for p + Fe (left panel) and p + Ta (right panel), Ta we will consider in the following as an example for a heavy window material. The data for both reactions are compared with calculations obtained with the Liège intra nuclear cascade (INC) code coupled with the GEMINI evaporation code referred to as INCL in the following, the LAHET (version 2.7d) and the HERMES code. In the case of the LAHET code two options were employed for the choice of the subsequent evaporation-fission models assuming the Coulomb barriers to be independent of (ORNL) or

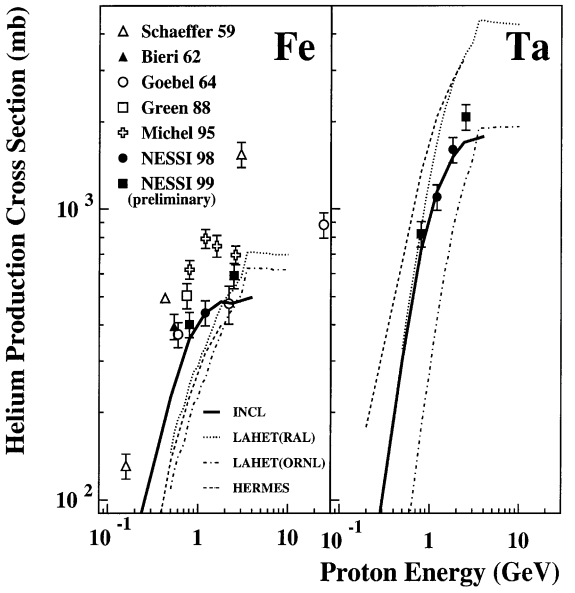

Fig. 2. Left panel: compilation [9] of p + Fe He-production cross-section data as a function of incident proton energy. The lines have been obtained with the indicated codes; LAHET(RAL) and LAHET(ORNL) refer to different evaporation-fission models, which are optionally available in LAHET. The NESSI-99 results are preliminary. Right panel: same for p + Ta.

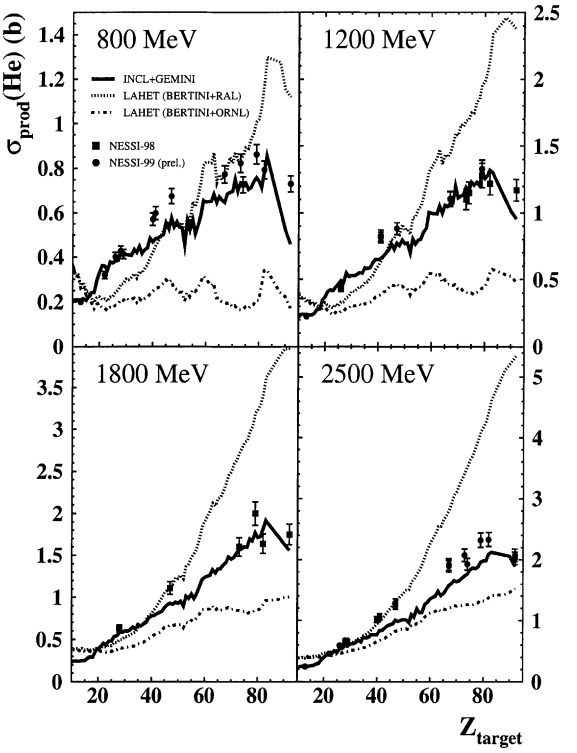

Fig. 3. Experimental [9,10] and calculated helium production cross-sections for 0.8, 1.2, 1.8, and 2.5 GeV proton induced reactions as a function of target atomic number Z_{target}. The thick solid line refers to INCL, the dashed-dotted or dotted line was obtained with the LAHET code employing an evaporation-fission model with constant Coulomb barriers (ORNL) or with excitation energy decreasing Coulomb barriers (RAL), respectively. Note the different scales of the left and right panels. The NESSI-99 results are preliminary.

to decrease (RAL) with excitation energy. Pre-equilibrium emission was taken into account. Further details of these codes and the employed parameters are described in [8–10].

The helium production cross-sections from NESSI are about a factor of 2 smaller for p + Fe and show in particular a different energy dependence than the data of Michel et al. [12]. The cross-sections as calculated with the LAHET and HERMES codes are somewhat smaller than the NESSI data in the case of p + Fe while for p + Ta HERMES and LAHET(RAL) predict larger cross-sections and LAHET(ORNL) smaller ones. The calculations with the INCL code are in good agreement with the data of both reactions: p + Fe and p + Ta.

The observed agreement between data and calculations with the INCL code is found also for all other targets including heavier targets as is shown in Fig. 3 for the helium production cross-sections. In contrast to this the LAHET code, with the two versions of evaporation models differing by assuming constant (dashed-dotted line) or with the excitation energy decreasing (dotted line) Coulomb barriers, under- or overestimate, respectively, the helium yield considerably. Since the Coulomb barriers for He-isotopes employed in LAHET(ORNL) are similar to the ones used in GEMINI and the excitation energy transferred during the INC in LAHET is larger than in INCL (as will be discussed in the next section) it is surprising that the predicted helium cross-sections are smaller than the ones calculated with INCL/GEMINI. This observation can be understood by the fact that (i) the Coulomb barriers for protons (at zero excitation energy) in LAHET are considerably smaller than in GEMINI [10] and (ii) at higher excitation energies an increasing fraction of the He-yield is due to the evaporation and subsequent decay of ^{5}He [10] which is taken into account in GEMINI in addition to the emission of the stable ^{3,4}He-isotopes.

2.3. Excitation and kinetic energy of HR

In addition to the above-described comparison of production cross-sections it was shown [9,10] that the distribution of excitation energy, residing in the nucleus after the fast INC step, is well described by the INCL code while the LAHET and HERMES codes predict considerably larger excitation energies. The excitation

energy E^* is correlated in two ways with the energy of the recoiling target-like nuclei. Both recoil and excitation energy increases with a decreasing fraction of the incident proton momentum carried off by prompt cascade particles (pions, n, p) emitted in the forward direction. The subsequent chain of evaporated particles induce a further, though smaller due the isotropic emission, increase of the recoil energy. While the mass loss due to the evaporation decreases the kinetic recoil energy of target-like residues. We exploit model calculations, which also reproduce the E^* distribution correctly, to obtain the recoil energy E_{HR} of residual nuclei of charge Z_{HR} and atomic number A_{HR}.

Recent measurements [11] of E_{HR} (A_{HR}) for $1 \cdot A$ GeV $^{208}Pb + H$ can furthermore be confronted directly with the results of such codes. LAHET as well as INCL reproduce reasonably well the functional dependence of the kinetic energy E_{HR} on the HR mass A_{HR}. The predictions, however, for the mean excitation energy $\langle E^* \rangle$ of the two INC codes differ up to factor of 2 as shown in Fig. 4 leading to residue mass distributions of much higher yield at smaller masses (with higher recoil energies) in LAHET than in the INCL simulations. Consequently the mean recoil energy will be considerably larger in the case of the LAHET code as will be shown below. It might be interesting to note that the mean nuclear excitation efficiency $\langle E^* \rangle / E_p$ in spallation reactions is quite small. It decreases from about 15% at a few hundred MeV to about 3% at 4 GeV for p + Fe and to 6% for the larger nucleus Ta.

Since the INCL code describes the helium cross-section and the excitation energy distributions and thus also the mean excitation energy very well we rely in the following on this code. The calculations for charged particle yields with the LAHET code will also be shown in Section 3.3 for comparison; they should be considered, however, with some caution.

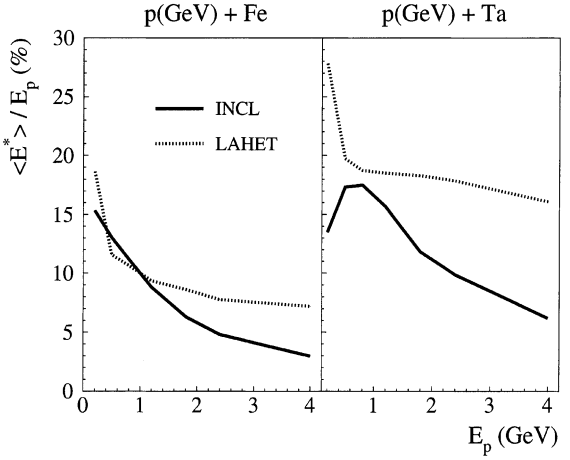

Fig. 4. Calculated mean fraction $\langle E^* \rangle / E_p$ of the incident proton energy E_p which is dissipated into excitation energy E^*. The INCL calculation is shown by the thick solid line, the one of LAHET by the dotted line.

3. Beam induced radiation damage in the window

As discussed in Section 2.1 and shown by the dotted line in Fig. 1 the neutron production per proton is increasing almost linearly between 1 and 4 GeV for typical spallation targets. What consequences does this observation have for the radiation damage induced in the target window? In order to produce the same number of neutrons at 4 GeV as at 1 GeV only about 1/4 of the incident proton current is needed. In the following we will investigate whether with the reduction of the proton current the induced damage due to helium gas and atom displacements decreases correspondingly and thus could result in an increase of window life times.

3.1. Helium gas production

For investigating the radiation damage induced by the deposition of helium gas of low mobility in a metallic material the helium production rate per produced neutron in a thick target (downstream of the window) can be considered as a good figure-of-merit: σ_{He}/n where σ_{He} is the helium production cross-section and n the number of neutrons produced in a thick target per incident proton.This ratio σ_{He}/n is shown in Fig. 5 for an Fe-like ($Z = 26$) window material (left panel) and as an example for a heavy material Ta with $Z = 73$ (right panel). In the case of Fe we observe a drastic decrease of helium production per produced neutron. From 1 to 4 GeV σ_{He}/n decreases from 17 to 6 mb/n. For a heavy material such as Ta the helium production is about 2.5 times larger than for Fe and furthermore a decrease with proton energy sets in only above about 3 GeV. Thus if helium gas production would be a critical parameter for beam induced radiation damage higher incident proton energies would clearly be more advantageous for steel windows.

3.2. Displacements per atom

As pointed out above the essential parameter describing the displacements produced per atom (dpa) is given by the damage or displacement cross-section σ_d. This quantity has been calculated by the relation

$$\sigma_d = \sigma_{inel} \times \frac{1}{n} \sum_{i=1}^{n} \sum_{j=1}^{M_i} N_{vac}(E_{ij}, Z_{ij}, A_{ij}), \quad (1)$$

where σ_{inel} is the total inelastic cross-section [13] of the spallation reaction, N_{vac} is the number of vacancies cre-

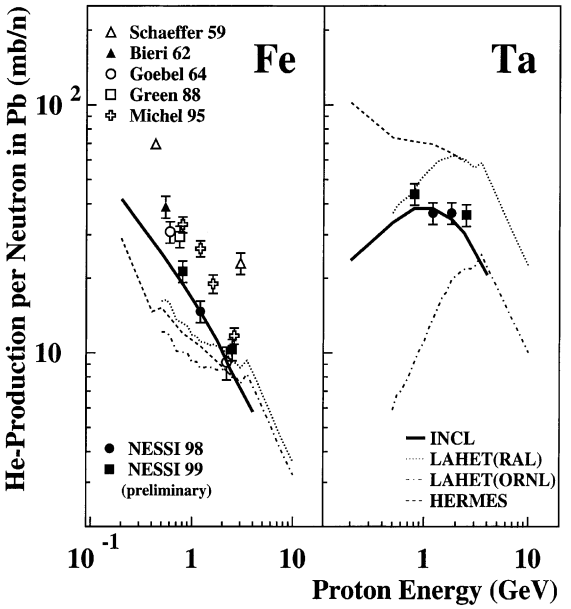

Fig. 5. Proton induced He-production cross-sections on Fe (left panel) and Ta (right panel) per produced neutron in a Pb spallation target in units of mb/n as a function of incident proton energy. The employed n/p has been deduced from the dotted line in Fig. 1.

ated by a charged particle of kinetic energy E_{ij}, charge Z_{ij}, and mass A_{ij}, M_i is the multipilicity of charged particles in the ith simulated reaction, and n is the total number of events as calculated with LAHET or INCL. In the following damage cross-sections have been calculated for H, He and HR. Fission was neglected here since the fission probability is too small for such a relatively light nucleus as Ta, whereas for Au and proton energies above 1 GeV the damage by fission fragments can amount to about 10% of the HR damage cross-section. Vacancy production due to elastic scattering of neutrons coming back from the neutron production target was not taken into account. It should be noted here, however, that the atom displacements induced in the window by neutrons from the spallation target can be up to twice as large as those induced by the proton beam [14].

For the calculations a window thickness of 2 mm was assumed. This thickness is only of importance for calculating the damage cross-section for energetic protons which have ranges comparable or larger than the window thickness. Since the probability to produce vacancies is largest towards the end of the range protons are contributing more effectively to the vacancy production in thicker windows.

The energy E_i, charge Z_i, and mass A_i (in Eq. (1)) of the particles have been obtained from the INCL code or LAHET code and used event-wise as input for the TRIM code [15] employing the Kinchin-Pease approximation [16] to follow secondary cascades of recoiling atoms. The employed effective threshold displacement energies derived from polycrystal damage rate measurements [17] were 40 eV for Fe and 88 eV for Ta.

The results as a function of incident proton energy are shown in Fig. 6 for an Fe- and a Ta-target. The thick and thin lines refer to results of the INCL and LAHET code, respectively. The top panels show the mean recoil energy $\langle E_{HR}\rangle$ after the prompt INC-cascade (dashed line) and after de-excitation by evaporation (solid line). The additional recoil energy transferred by the evaporated particles to the HR is relatively small for Fe while for Ta it amounts up to 20%. The corresponding dependence of the mean charge loss of HR $\langle \Delta Z_{HR}\rangle = \langle Z_{HR}\rangle - Z_T$,with $\langle Z_{HR}\rangle$ and Z_T the mean atomic number of HR and target atomic number (26 for Fe and 73 for Ta) before (dashed line) and after (solid line) evaporation is shown in the second row of panels.

The third row of panels in Fig. 6 shows the essential quantity of interest for radiation damage, namely the damage cross-section σ_d in barns. The relative effect of

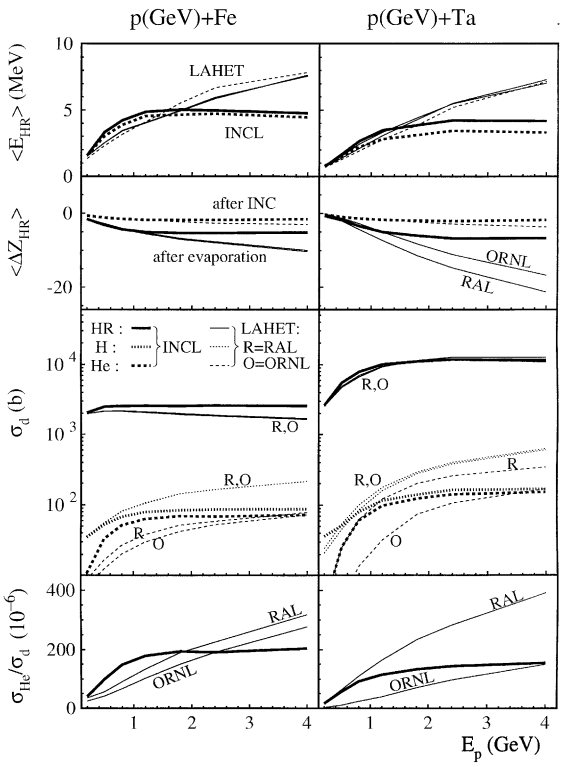

Fig. 6. With the code INCL (thick lines) and LAHET(RAL, ORNL) (thin lines) calculated proton energy dependence of the mean recoil energy $\langle E_{HR}\rangle$; mean charge loss $\langle \Delta Z_{HR}\rangle$ after INC (dashed) and after INC plus evaporation (solid line); damage cross-section σ_d of hydrogen (H) , helium (He), and HR; He/dpa ratio σ_{He}/σ_d for beam exposed Fe (left) and Ta (right) windows with a thickness of 2 mm, see also text.

the various reaction products in a 2 mm thick window is indicated. The slightly larger damage cross-sections observed for hydrogen isotopes than for helium isotopes is due to the 5–7 times larger (INCL) hydrogen yield compared to helium. The damage cross-section is, however, completely dominated by the HR.

The essential point to make here is the finding that the damage cross-sections are almost constant above about 1–2 GeV of proton energy: 2.8×10^3 b for Fe and 12×10^3 b for Ta. For one year of operation of ESS with an integrated proton flux of $\phi t = 1.9 \times 10^{22}$ p/cm^2 this corresponds to 55 and 230 displacements per atom ($\mathrm{dpa} = \sigma_d \phi t$) for Fe and Ta, respectively. These numbers do not include neutron induced displacements which can be, however, of the same order of magnitude [14].

As pointed out in Section 1 radiation damage induced by spallation reactions is particularly characterized by a large He/dpa ratio compared to 0.5×10^{-6} observed in fission reactors. The ratio He/dpa of helium production per atom to displacements per atom is given by $\mathrm{He/dpa} = \sigma_{\mathrm{He}}/\sigma_d$. The thus obtained ratio is shown in the bottom two panels of Fig. 6. We observe that the He/dpa ratio increases with proton energy up to about 1–1.5 GeV while for higher energies it is essentially constant and approaches 200×10^{-6} for Fe and 140×10^{-6} for Ta.

3.3. Comparison of different codes: INCL/LAHET

Since the LAHET code was employed extensively for simulation calculations of the target station of spallation neutron sources, it is of particular interest to compare the results from INCL with those of LAHET.

The predictions of LAHET and INCL for the helium gas production per produced neutron (see Fig. 5) are similar for Fe concerning the energy dependence as well as the absolute values. For a heavy material such as Ta the LAHET(RAL) code strongly overestimates the helium gas production while LAHET(ORNL) underestimates it in particular for proton energies below 3 GeV.

The mean recoil energy $\langle E_{\mathrm{HR}} \rangle$ as calculated with LAHET reaches considerably larger values, 8 instead of 5 MeV for Fe, than obtained with INCL at proton energies above about 2 GeV in agreement with the finding of larger mean excitation energies as shown in Fig. 4. Thus one would expect larger damage cross-sections, about 10% as obtained from TRIM calculations, to be predicted by LAHET. The damage cross-section calculated with LAHET are, however, smaller for Fe (2 kb) and about the same for Ta compared to the ones obtained with the INCL code. The reason for this unexpected finding is due to the considerably smaller mean charge $\langle Z_{\mathrm{HR}} \rangle$ and mass $\langle A_{\mathrm{HR}} \rangle$ of the HR in the case of LAHET compared to INCL. The lower charge of the lighter HR reduces the probability to produce vacancies despite the larger recoil energy. In the case of Ta both effects cancel each other almost completely . Damage or displacement cross-sections for Fe as calculated with the HETC-SID code are very similar to the present LAHET-TRIM results in absolute numbers as well as proton energy dependence [18].

In summary, both codes result in almost the same and constant damage cross-sections while He/dpa is strongly increasing with proton energy in the case of the two versions of the LAHET code (RAL and ORNL) while it is almost constant for the INCL code. The observed approximately constant damage cross-section above about 1 GeV means that the induced damage decreases with increasing incident proton energy for the same amount of neutrons produced in a thick target as discussed above.

4. Conclusions

In summary we conclude that for the same amount of neutron production in a spallation target the proton beam current can be decreased almost linearly with increasing proton energy above about 1 GeV. With this reduction of beam current the radiation damage induced in Fe-like window materials due to helium gas production and atom displacements reduces also almost proportionally. While for windows made from heavier material such as Ta a similar decrease as for Fe can be expected only for proton energies above about 3 GeV. Since in the present work only proton and no neutron induced displacement cross-sections were calculated the above-discussed decrease of dpa with proton energy will be less steep depending on the atom displacements induced by the constant neutron flux coming back from the neutron production target.

The damage cross-sections calculated with the LAHET and INCL codes were shown to be very similar despite considerable differences in other observables. For the He/dpa ratio, however, the two codes differ considerably both in absolute numbers as well as in the energy dependence. Above about 1 GeV the electronic stopping power is nearly constant and thus the heating of the window decreases with the reduction of beam current as well. Though it might be advantageous with respect to the induced radiation damage to employ higher proton energies, there are off course also disadvantages such as for instance the increased yield of energetic neutrons from the production target requiring larger shielding.

Acknowledgements

This work was partly supported by the German HGF-Strategiefonds project R&D for ESS, the French

GEDEON project, and the EU-TMR project ERB-FMRXCT980244.

References

[1] The European Spallation Source Study, vol. III, The ESS Technical Study, Report ESS-96-53-M, 1996.
[2] Spallation Neutron Source at Oak Ride, TN, USA, http://www.sns.gov/documentation/pubs.htm.
[3] H. Ullmaier, F. Carsughi, Nucl. Instrum. and Meth. B 101 (1995) 406.
[4] H. Ullmaier, E. Camus, J. Nucl. Mater. 251 (1997) 262.
[5] S.A. Maloy et al., in: Third International Topical Meeting on Nuclear Applications of Accelerator Technology, Long Beach, CA, 14–18 November 1999, p. 541.
[6] A. Letourneau et al., Nucl. Instrum. and Meth. B 170 (2000) 299.
[7] D. Hilscher et al., Nucl. Instrum. and Meth. A 414 (1998) 100.
[8] D. Filges et al., to be published.
[9] M. Enke et al., Nucl. Phys. A 657 (1999) 317, and references [4–8, 27–34] therein.
[10] C.-M. Herbach et al., in: Proceedings of SARE-5 Meeting, 17–21 July 2000, OECD, Paris, France.
[11] W. Wlazlo et al., Phys. Rev. Lett. 84 (2000) 5736.
[12] R. Michel et al., Nucl. Instrum. and Meth. B 103 (1995) 183.
[13] H. P. Wellisch, D. Axen, Phys. Rev. C 54 (1996) 1329, revised by R.E. Prael, M.B. Chadwick, Los Alamos National Laboratory, Report LA-UR-97-1745, 1997.
[14] M.H. Barnett, M.S. Wechsler et al., these Proceedings, p. 54.
[15] J.P. Biersack, L.G. Haggmark, Nucl. Instrum. and Meth. 174 (1980) 257.
[16] G.H. Kinchin, R.S. Pease, Rep. Prog. Phys. 18 (1955) 1.
[17] P. Jung, Landolt-Börnstein, New Series III/25 (1991) 1, and references therein.
[18] D. Filges et al., Report ESS 96-45-T, 1996.